Nanotechnology **22** (2011) 085702 (8pp) doi:10.1088/0957-4484/22/8/085702

Optical properties of heavily doped GaAs nanowires and electroluminescent nanowire structures

A Lysov[1], M Offer[1], C Gutsche[1], I Regolin[1], S Topaloglu[2], M Geller[1], W Prost[1] and F-J Tegude[1]

[1] Center for Nanointegration Duisburg-Essen, University of Duisburg-Essen, D-47048 Duisburg, Germany
[2] Department of Electronics Engineering, Maltepe University, Marmara Eğitim Köyü, 34857, Maltepe, Istanbul, Turkey

E-mail: andrey.lysov@uni-due.de

Received 8 September 2010, in final form 30 November 2010
Published 17 January 2011
Online at stacks.iop.org/Nano/22/085702

Abstract

We present GaAs electroluminescent nanowire structures fabricated by metal organic vapor phase epitaxy. Electroluminescent structures were realized in both axial pn-junctions in single GaAs nanowires and free-standing nanowire arrays with a pn-junction formed between nanowires and substrate, respectively. The electroluminescence emission peak from single nanowire pn-junctions at 10 K was registered at an energy of around 1.32 eV and shifted to 1.4 eV with an increasing current. The line is attributed to the recombination in the compensated region present in the nanowire due to the memory effect of the vapor–liquid–solid growth mechanism.

Arrayed nanowire electroluminescent structures with a pn-junction formed between nanowires and substrate demonstrated at 5 K a strong electroluminescence peak at 1.488 eV and two shoulder peaks at 1.455 and 1.519 eV. The main emission line was attributed to the recombination in the p-doped GaAs. The other two lines correspond to the tunneling-assisted photon emission and band-edge recombination in the abrupt junction, respectively. Electroluminescence spectra are compared with the micro-photoluminescence spectra taken along the single p-, n- and single nanowire pn-junctions to find the origin of the electroluminescence peaks, the distribution of doping species and the sharpness of the junctions.

(Some figures in this article are in colour only in the electronic version)

1. Introduction

The miniaturization of devices remains one of the main approaches used in microelectronics for the creation of systems with an enhanced functionality [1]. Shrinkage of the device size makes use of the expensive 'top down' techniques, making clear that new cheaper 'bottom-up' concepts are necessary to overcome the limitations of conventional lithographic methods [2].

III/V semiconductor nanowires are interesting candidates for the bottom-up fabrication of nano-photonic [3–6] and photo-voltaic [7] devices. They offer the possibility for the monolithic integration of compound semiconductors with mature silicon technology [6, 8]. Nanowire array light emitting diodes (LEDs) were reported to possess higher light extraction efficiency than conventional broad area LEDs due to their large sidewall surface area [9].

The vapor–liquid–solid (VLS) nanowire growth mode used in this work utilizes a gold seed as a catalyzer for the nanowire growth [10]. It combines a high growth rate at low temperatures, where conventional layer growth is suppressed, with a localization of the nanowire at the gold seed position.

The important key features for the fabrication of a nanowire LED are a control of both nanowire morphology and doping. This way the realization of axially doped nanowire pn-junctions with specific electroluminescent (EL) properties becomes feasible.

The first axial GaAs nanowire based LEDs were realized in 1992 using top-contacted nanowire arrays grown under

alternating silicon and carbon supply during the growth on n-GaAs substrate [11, 12]. Since carbon has a low solubility in gold and nanowires were heavily tapered, pn-junctions may have been realized not within the nanowire but rather between a carbon-doped shell grown via the conventional vapor–solid (VS) growth mode and a silicon-doped GaAs substrate.

Nanowire EL structures have already been demonstrated in axial pn-junctions [3, 5] as well as in axial quantum well structures [4] grown by the VLS mechanism in InP.

The VLS growth mechanism has a significant influence on the incorporation of the doping species.

In recent reports a grading of the nanowire doping was observed by conductivity measurements on GaAs nanowires doped with zinc and tin due to memory effects in the growth seed [13, 14]. The carrier concentration was increased towards the nanowire tip, leading to an increased conductivity. The sample preparation for electrical measurements requires definition of the position for every nanowire with consequent contacting via electron beam lithography, which is quite time consuming. In addition, electrical measurements do not allow determination of the doping distribution with high spatial resolution. For that reason the development of new methods for the investigation of the doping distribution along the nanowire length and its influence on the sharpness of the pn-junction and the EL properties of the diode is an important goal.

We present the optical properties of single axial pn-GaAs nanowires and nanowire EL structures grown on (111)B GaAs substrates by metal organic vapor phase epitaxy (MOVPE) in the VLS growth regime based on Au seed particles.

Micro-photoluminescence (μ-PL) spectroscopy is used as a direct means to measure the band gap energy as a function of the carrier concentration along the nanowire length and to draw conclusions about the distribution of doping species along the single nanowire pn-junctions.

To compare the luminescent properties of the single pn-junctioned nanowires with those from sharp nanowire based pn-junctions grown under the same conditions, we have fabricated arrayed nanowire top-contacted pn-diodes. The sharp pn-junctions were realized with an n-type-doped GaAs substrate serving as the n-type part of the diode and zinc-doped non-tapered nanowires serving as the p-type part.

The EL spectra of the nanowire arrayed LEDs at low and room temperature are presented and compared with μ-PL-and EL-spectra of single nanowire pn-junctions.

2. Experimental details

Nanowires were grown via VLS growth mode by use of low pressure MOVPE (50 mbar).

Trimethylgallium (TMGa), tertiarybutylarsine (TBAs), diethylzinc (DEZn) and tetraethyltin (TESn) were used as group-III and group-V precursors as well as p-type and n-type doping precursors, respectively. The total gas flow of 3.3 l min^{-1} was adjusted within the reactor, with nitrogen as carrier gas and hydrogen as source gas.

As templates for the nanowire growth, polydisperse nanoparticles were used. The polydisperse nanoparticles were obtained from a nominally 2.5 nm thin Au-layer during the annealing step of 600 °C for 5 min before growth. Annealing was carried out under TBAs flow with a molar fraction of $\chi_{\text{TBAs}} = 3.16 \times 10^{-4}$.

The nanowire growth was initiated by introduction of TMGa ($\chi_{\text{TMGa}} = 1.32 \times 10^{-4}$) into the reactor at an elevated temperature of 450 °C to promote the nucleation of the wire and reduce kinking effects at the beginning of the growth [15]. After a growth of the intrinsic nanowire stump for 3 min, the temperature was lowered to 400 °C. The p-part of the nanowire was grown under supply of DEZn with a molar fraction of $\chi_{\text{DEZn}} = 5.72 \times 10^{-7}$, corresponding to the mean hole concentration of 2×10^{19} cm^{-3} in the nanowire [13]. For n-doped nanowires, TESn was used as a doping precursor with a molar fraction of $\chi_{\text{TESn}} = 1.05 \times 10^{-5}$, corresponding to the mean electron concentration of 1×10^{18} cm^{-3} in the nanowire [14]. The carrier concentrations in the nanowires were determined by the mobility versus carrier concentration model, which is thoroughly discussed in [13, 14]. After growth, the sample was cooled down to room temperature under arsenic stabilization. The nanowire pn-junctions were grown by switching the doping precursors from DEZn to TESn without any growth interruption. More details about the growth, morphological and electrical properties of single nanowire pn-junctions can be taken from [16].

For the growth of arrayed nanowire pn-junctions, n-doped (111)B GaAs substrate with a carrier concentration of $n = 1.5 \times 10^{18}$ cm^{-3} was used. Polydisperse Au-seeds were produced by annealing of a 2.5 nm thick Au-layer, which was pre-patterned via optical lithography. P-doped GaAs nanowires were grown with the above parameters without an intrinsic stump. DEZn has been supplied into the reactor for 2 min at 400 °C before growth to pre-saturate an Au seed with zinc and facilitate an abrupt junction formation between substrate and the nanowire.

The substrate serving as an n-part of the junction was contacted by Ge/Ni/Ge/Au metallization and annealed at 400 °C for 30 s to achieve an ohmic contact behavior.

A durimide based technology was adopted to contact free-standing nanowires. A durimide layer was deposited on the free-standing nanowires by spin-on coating and formed an isolator separating the top contact from the substrate. Pt/Ti/Pt/Au metallization was patterned to form the ohmic top-contacts to the p-doped nanowires.

For photoluminescence characterization, nanowires were scratched off the substrate, dispersed in isopropyl alcohol and deposited on a Si substrate. For electrical and EL measurements as-grown pn-doped nanowires were transferred to pre-patterned insulating carriers and contacted by electron beam lithography and the evaporation technique. Pt/Ti/Pt/Au was used to contact the p-GaAs nanowire part. To achieve ohmic contact behavior, rapid thermal annealing was carried out at 360 °C for 30 s. Pd/Ge/Au annealed for 30 s at 280 °C was used as an ohmic contact for the n-doped nanowire part.

μ-PL and EL measurements were carried out in a liquid helium cooled continuous flow optical cryostat fitted with an XY piezo-driven scanning stage. Optical excitation was made by a CW Nd:YVO4 laser with $\lambda = 532$ nm. For μ-PL measurements, the optical resolution of the setup is given by

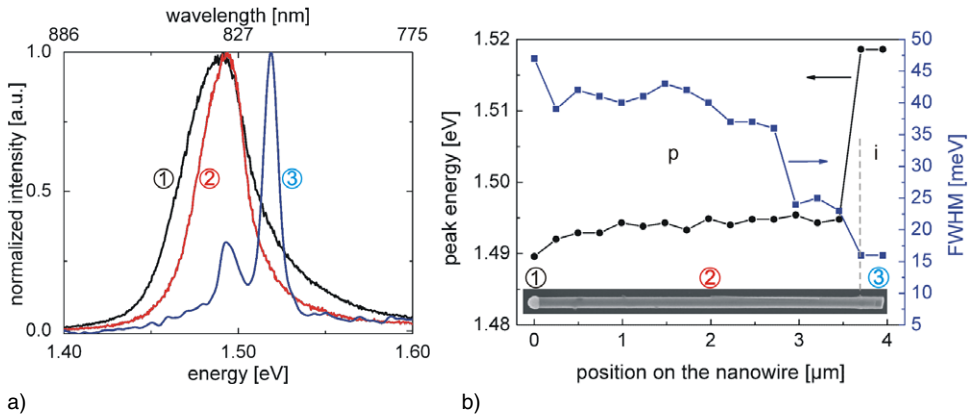

Figure 1. (a) μ-PL spectra taken at different positions along the Zn-doped GaAs nanowire. Positions on the nanowire are denoted by numbers in the inset of (b). (b) Peak energy and the FWHM along the nanowire length. The inset shows a scanning electron microscopy (SEM) micrograph of the investigated nanowire.

the diameter of the focused laser spot (<1 μm) on the sample. An aperture determines the field of view for EL measurements, which has been 5 μm in our measurement. The measurements were carried out using a Czerny–Turner monochromator (focal length $f = 500$ mm) with an L_{N2}-cooled charge-coupled device as a detector.

3. Results and discussion

3.1. Photoluminescence

To investigate the optical properties of the p-doped GaAs:Zn nanowires μ-PL spectra were taken at a temperature of 6 K at different locations along the nanowire length. The optical power density was 8×10^4 W cm^{-2}. Figure 1(a) shows μ-PL spectra taken from a 125 nm thick nanowire at different positions. The corresponding positions are indicated by numbers in the inset in figure 1(b). The peak energy as well as its line shape change along the nanowire length. At the nominally undoped nanowire stump (position 3) the main peak has a maximum at 1.519 eV and originates from a free-exciton recombination. In the case of nanowires, the free-exciton peak is broader than for the bulk samples (width at half maximum (FWHM) <5 meV at liquid helium temperature). Peak broadening appears because of the encounters between excitons and imperfections such as a nanowire surface or impurities (Au) as well as due to possible strain present in the nanowire stump. The second peak at 1.493 eV originates from the p-doped nanowire part, which was excited by the same laser spot as well. As the laser spot is moved towards the nanowire tip the line corresponding to the p-doped region becomes more intensive and finally dominates the whole spectrum as can be seen on the spectra for the positions 1 and 2.

In figure 1(b), the peak position and its FWHM are presented. The peak position shifts slightly to lower energy (from 1.495 to 1.489 eV) towards the nanowire tip. A significant broadening of the line appears towards the nanowire tip and the peak intensity is decreased, which is not presented here.

We explain this behavior by the gradient of the degenerate p-doping along the wire length. The impact of increasing doping degeneration on photoluminescent properties has already been reported in [17, 18] for heavily Zn-doped GaAs bulk samples. The authors attributed the peak to the recombination of the electrons with holes via acceptor states above the valence band edge, which form a broadened acceptor band in the heavily p-doped semiconductor. This assumption is supported by the fact that the energy difference between this line and the exciton peak nearly corresponds to the binding energy of the Zn-acceptor in GaAs of $E_A = 24$ meV. An increasing doping concentration results in the broadening of the acceptor band and leads therewith to an increased line width of the peak. This band broadening, which is stronger towards the conduction band, explains a slight peak shift to the lower energy.

n-doped GaAs nanowires were characterized via μ-PL measurements to investigate the influence of the graded doping profile on the optical properties of the wires.

Figure 2(a) shows μ-PL spectra of a tin-doped GaAs nanowire of 120 nm diameter at different positions. The positions corresponding to the spectra are indicated by numbers on the inset in figure 2(b). The spectra were taken at a temperature of 9 K under an optical excitation density of 4×10^3 W cm^{-2}. Due to the high PL signal intensity, the power density was chosen lower than for p-doped nanowires.The peak energy as well as its line shape change as the laser spot is scanned along the nanowire. At the intrinsic nanowire stump (position 3) the main peak was observed with a maximum at 1.519 eV originating from a free-exciton recombination. This line is superimposed on the broad peak with a maximum at 1.557 eV stemming from the n-doped nanowire part. As the nanowire is scanned towards the nanowire tip, the line corresponding to the nanowire stump disappears and a peak originating from the n-doped region shifts towards higher energies (positions 1 and 2). At the same time a substantial broadening of the peak appears, as can be seen in the FWHM curve in figure 2(b).

We attribute this effect to the Burstein–Moss shift of the PL peak observed in heavily doped n-GaAs samples [18].

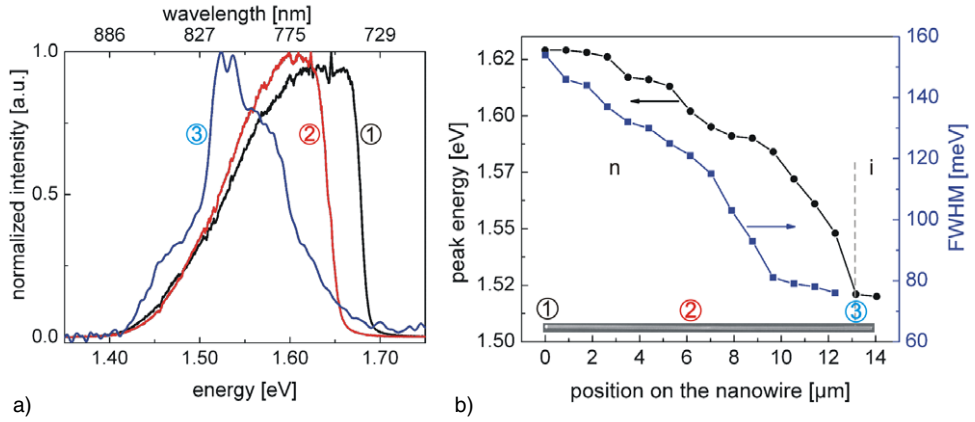

Figure 2. (a) μ-PL spectra taken at different positions along the Sn-doped GaAs nanowire. Positions on the nanowire are denoted by numbers in (b). (b) Peak energy and the FWHM along the nanowire length. The inset shows an SEM micrograph of the investigated nanowire.

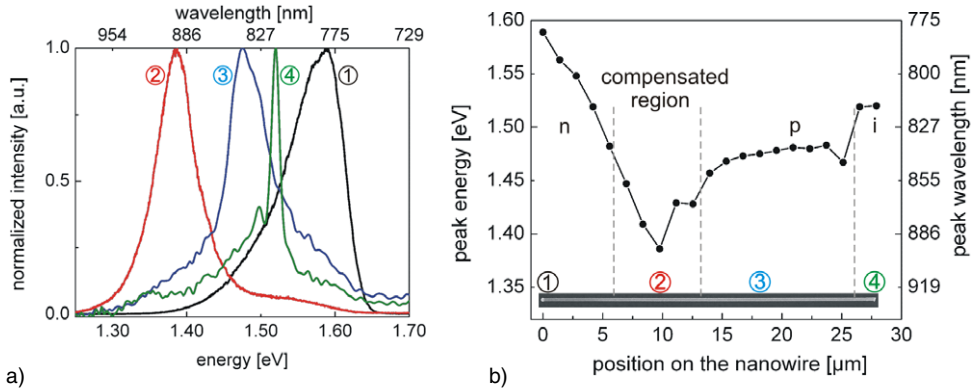

Figure 3. (a) μ-PL spectra taken at different positions along the pn-junctioned GaAs nanowire. Positions on the nanowire are denoted by numbers in (b). (b) Peak energy along the nanowire length. The SEM image of the investigated nanowire is shown in the inset.

Since the nanowires are highly doped, the Fermi level is located inside the conduction band. With a further increase of carrier concentration towards the nanowire tip, a band filling with electrons is taking place, which manifests itself in the Fermi level shift and consequently in the shift of PL peak to the higher energies [19].

The high-energy edge of the peak has an abrupt cutoff at a photon energy corresponding to the separation between the quasi-Fermi levels of electrons and holes. The low-energy edge of the emission spectrum represents a convolution of the states below the quasi-Fermi levels linked by the same photon energy and possessing, therefore, a mild slope. For n-doped GaAs nanowires the Burstein–Moss shift overrules a band gap narrowing, taking place at the same time. The reason for this is that the density of states in the conduction band of GaAs is an order of magnitude lower than in the valence band.

The developed μ-PL investigation method was applied to GaAs nanowire pn-junctions grown with a direct switching of doping precursors to analyze the sharpness of the fabricated junction.

Figure 3(a) shows μ-PL spectra taken at the pn-doped GaAs nanowire of 150 nm diameter at different positions. The spectra were taken at a temperature of 9 K under an optical excitation density of 8×10^4 W cm^{-2}. The positions corresponding to the spectra are indicated by numbers on the inset in figure 3(b).

Four regions can be recognized on the plot of the peak energy along the nanowire length. At the intrinsic nanowire stump (position 4) an exciton peak at 1.519 eV is observed (spectrum 4 in figure 3(a)). As the laser spot moves further to the p-doped nanowire part, the main peak shifts to the range 1.47–1.49 eV (figure 3(b) and spectrum 3 in figure 3(a)) characteristic for the graded p-doped GaAs nanowires as discussed above. In the n-doped area close to the nanowire tip the position of the PL peak was measured in the range between 1.48 and 1.58 eV, which corresponds to the results for the n-doped nanowires, discussed above.

In the area between n- and p-doped nanowire parts a PL peak position between 1.38 and 1.48 eV is observed (figure 3(b) as well as spectrum 2 in figure 3(a)). These line energies correspond neither to p- nor to n-doped nanowires. The emission lines with these energies were reported in [20] for compensated GaAs samples. Therefore, we attribute these lines to the compensated region located in the area of the pn-junction. Due to the memory effect of the growth seed, some zinc is still present in gold after switching of the doping precursors from DEZn to TESn, yielding a region where both doping species are present. An origin of such lines is

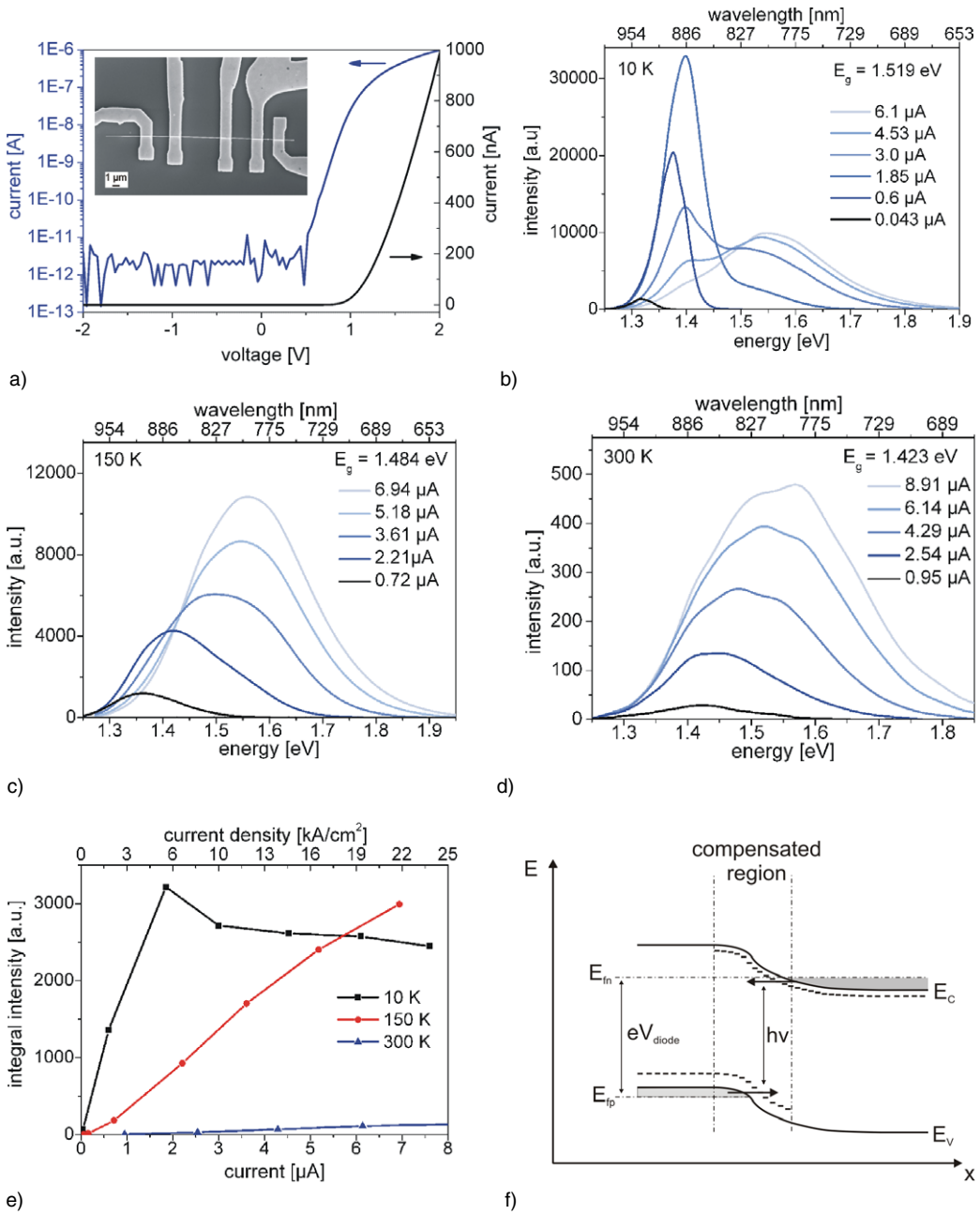

Figure 4. (a) $I(V)$ characteristics of the single GaAs nanowire pn-diode in semi-logarithmic (left axis) and linear (right axis) plots at room temperature. The inset shows an SEM micrograph of the contacted nanowire-diode. (b)–(d) EL spectra taken at the single pn-junctioned GaAs nanowire for different excitation levels at 10 K, 150 K and 300 K, respectively. The band gap of GaAs at corresponding temperatures is indicated in the figures. (e) Integral emission intensity versus current at different temperatures. Current density through the pn-junction is plotted on the upper axis. (f) Model of a band structure for a diode with a compensated region biased in the forward direction with a voltage V_{Diode}. E_{fn} and E_{fp} are the electron and hole quasi-Fermi levels, respectively. The tunneling-assisted radiative transition in the compensated region is indicated by an arrow.

described in [19] and is illustrated in figure 4(f). The emission is believed to come from the tunneling-assisted transitions between spatially separated degenerate donator and acceptor states, so that emission lines with energy much lower than the band gap may appear.

3.2. Electroluminescence

To investigate the electroluminescence properties of single nanowire pn-diodes, the contacted nanowire samples (inset in figure 4(a)) were glued to the chip-carrier and wire bonded. The single nanowire pn-junction with a diameter of 200 nm and a diode-like $I(V)$ characteristic (figure 4(a)) was excited by a constant current in the forward direction while emissions spectra were measured. The diode had a diffusion voltage of approximately 1.3 V and an ideality factor of 3 in a low voltage range under the measurement conditions. The poor ideality factor of the investigated diode is explained by high parasitic serial resistance, which was calculated to be $8\times10^5\ \Omega$. This serial resistance can be taken into account according to

$I = I_o \exp[(V - R_s I)/nkT]$, which results in an intrinsic ideality factor of 2.3. This value gives evidence for a defect related recombination of minority carriers in a junction region at low currents. An inverse current in the low picoampere range limited by the measurement setup was measured. An on–off ratio I_{max}/I_{rev} was estimated to be 10^{10}, demonstrating good rectifying performance of a diode. Concerning the on–off ratio, axial pn-junctions are advantageous over both radial pn-junctions and free-standing top-contacted nanowire junctions embedded in an isolator, which typically exhibit lower on–off ratios.

Figure 4(b) shows EL spectra from a single pn-junctioned nanowire taken at 10 K under different excitation currents.

At low currents the emission peak has a maximum at 1.32 eV (figure 4(b)). For higher injection current the peak shifts to 1.4 eV and its intensity increases until an injection current of 1.85 μA. The observed peak energy is unusual for exciton-and tunneling-assisted photon emission observed in abrupt pn-junctions [21], which occurs at higher energies at liquid helium temperature. On the other hand the energy of the observed emission line corresponds to those observed in the compensated region via photoluminescence in pn-GaAs nanowires, which is described above. For that reason we attribute the peak to the tunneling-assisted transition between the donor and acceptor band, taking place in the compensated region of the pn-junction (figure 4(f)). This assumption of radiative tunneling is supported by the shift of the emission peak to higher energies with an increasing excitation current [22]. This shift is expected for tunneling-assisted transitions and is explained by shifts of the quasi-Fermi levels with respect to each other.

The slope of the band structure at the junction flattens at higher bias voltages, causing a reduction of tunneling probability and a decrease of the tunneling emission. For this reason the tunneling-assisted emission peak diminishes for high injection levels and becomes dominated at 4.5 μA by band-edge emission, appearing at 1.51 eV for 10 K.

Scattering of free carriers by phonons increases at higher temperatures. This lowers the tunneling probability and makes it more difficult to distinguish between two emission mechanisms. Tunneling-assisted emission is still observed for low injection currents at 150 K (0.72 and 2.21 μA curves in figure 4(c)). At room temperature broad band–band emission dominates the whole spectrum even for low injection currents (figure 4(d)). The population of states above the quasi-Fermi level increases with temperature and explains broadening of the emission peak at the high-energy side while the low-energy tail stays saturated.

The dependence of the integral emission intensity on the injection current is shown in figure 4(e). While at 150 and 300 K the integral EL intensity increases linearly with current, a saturation of integral intensity is observed at 10 K from 1.85 μA. Saturation of an integral intensity for high injection levels at 10 K indicates that tunneling-assisted photon emission is a more efficient radiative process than band–band emission at low temperature. Band–band emission takes place in the adjacent p-doped nanowire part rather than in the junction region and comes along with a high rate of non-radiative recombination due to the high doping in the nanowire.

To improve the sharpness of nanowire pn-junctions, arrayed nanowire EL structures were fabricated. A pn-junction was formed between p-doped non-tapered GaAs nanowires grown on n-doped (111)B GaAs substrate, as shown in the schematic in figure 5(a). Contacted arrays contained approximately 50 nanowires. Durimide technology was adopted to form an isolator separating the substrate from the top contact. Using oxygen plasma, the durimide was etched down until the whisker top became free. A SEM image of the fabricated structure is presented in figure 5(a). The fabricated pn-structure possessed a typical diode-like $I(V)$ characteristic with quite high forward currents of about 2 mA at 2 V, and had an ideality factor of 1.5 in the low voltage range at room temperature (figure 5(b)).

Figures 5(c) and (d) present the EL spectra of the fabricated pn-diode. Arrayed nanowire EL structures demonstrate at 5 K a strong EL peak at 1.488 eV, which is attributed to the electron–acceptor band recombination in the p-doped GaAs wires. Besides the main peak, two shoulder peaks at 1.45 and 1.52 eV are present. We attribute the peak at 1.45 eV to tunneling-assisted photon emission, observed in abrupt GaAs pn-junctions at this energy [21]. The peak at 1.52 eV corresponds to the GaAs band gap at 5 K and originates from the band–band recombination at the junction. At room temperature one main peak was observed at 1.427 eV, only. This line energy corresponds to the band gap of GaAs at room temperature and is therefore attributed to the band-edge emission due to thermal injection. Since the peak was very broad neither of the other lines could be distinguished.

4. Conclusion

We have investigated the optical properties of single heavily doped p-GaAs, n-GaAs as well as pn-GaAs nanowires via micro-photoluminescence. A strong impact of the graded doping distribution along the nanowire length on the optical properties of nanowires was found. An emission line at 1.495 eV was observed in heavily p-doped GaAs nanowires, and was attributed to electron–hole recombination via the acceptor band. An increasing hole concentration towards the nanowire tip caused a line shift to lower energies (1.489 eV) and its broadening along the nanowire length.

The Burstein–Moss shift of the emission line to higher energies (from 1.55 to 1.62 eV) was observed in heavily n-doped GaAs nanowires along the nanowire length due to the increase of doping and resulting band filling towards the nanowire tip.

The presence of the compensated region due to the memory effect of the growth seed was found in the single GaAs nanowire pn-junctions via μ-PL measurements.

Electroluminescence in single axial GaAs pn-junctions was demonstrated for the first time. An emission line was observed at 1.32 eV and shifted to 1.4 eV with an increasing injection current at 10 K. The line was attributed to the tunneling-assisted transition between donor and acceptor states, taking place in the compensated region of the diode. At high injection levels, band–band transition dominates the EL spectrum. At higher temperatures broad band–band transition sets in even for low injection levels and dominates the spectrum.

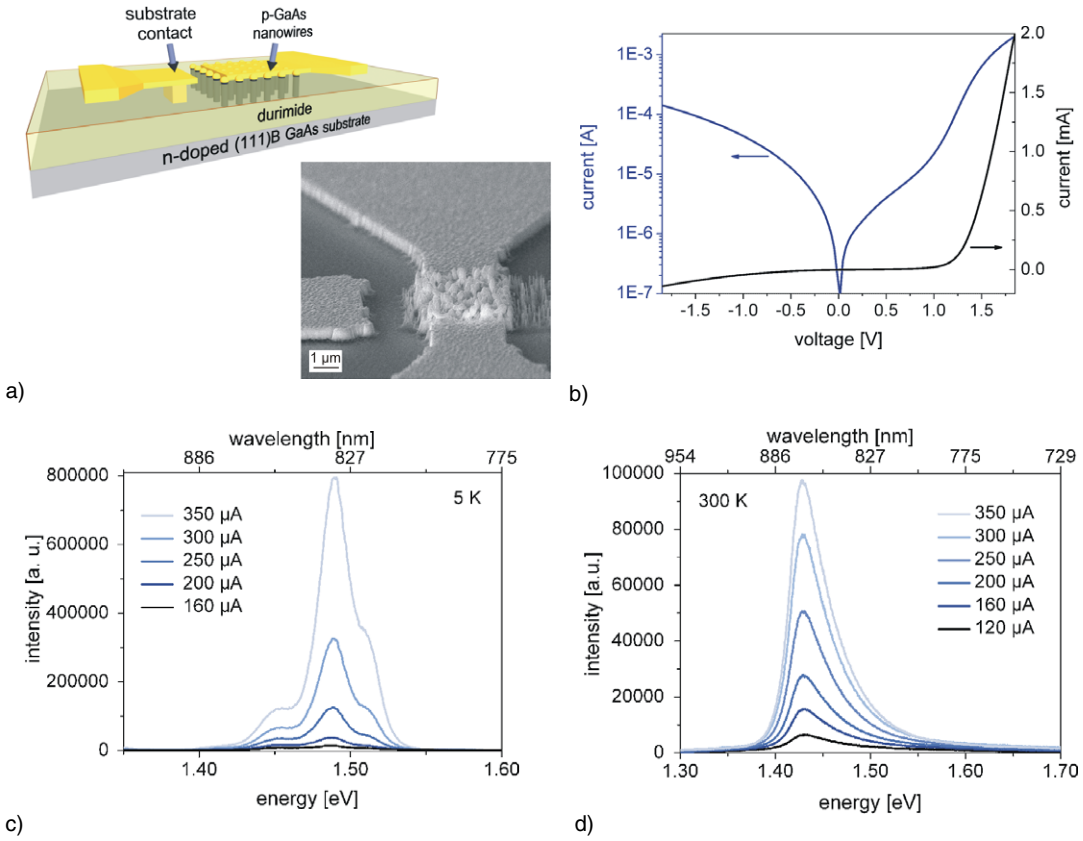

Figure 5. (a) Schematics and an SEM micrograph of the fabricated arrayed nanowire LED. (b) $I(V)$ characteristics of the arrayed nanowire LED in semi-logarithmic (left axis) and linear (right axis) plots. (c) EL spectra of the arrayed nanowire LED taken at 5 K. (d) EL spectra of the arrayed nanowire LED taken at 300 K.

Arrayed nanowire EL structures with an abrupt pn-junctions at the nanowire–substrate interface were fabricated from the free-standing p-doped nanowires on the n-doped substrate. Strong electroluminescence was demonstrated at both 5 K and room temperature. The main emission line at 1.488 eV was attributed to recombination in the p-doped GaAs wires and two shoulder peaks at 1.45 and 1.52 eV were attributed to tunneling-assisted photon emission and the band–band recombination at the abrupt junction, respectively. At room temperature a broadened peak at 1.427 eV originating from band-edge emission was observed.

Acknowledgments

We gratefully acknowledge partial financial support by the Sonderforschungsbereich SFB 445 and European project NaSol within the Ziel2.NRW program.

References

[1] 2009 International Technology Roadmap for Semiconductors http://www.itrs.net
[2] Bohr M T 2002 Nanotechnology goals and challenges for electronic applications *IEEE Trans. Nanotechnol.* **1** 56–62
[3] Gudiksen M S, Lauhon L J, Wang J, Smith D C and Lieber C M 2002 Growth of nanowire superlattice structures for nanoscale photonics and electronics *Nature* **415** 617–20
[4] Minot E D, Kelkensberg F, van Kouwen M, van Dam J A, Kouwenhoven L P, Zwiller V, Borgström M, Wunnicke O, Verheijen M A and Bakkers E P A M 2007 Single quantum dot nanowire LEDs *Nano Lett.* **7** 367–71
[5] Borgström M T, Norberg E, Wickert P, Nilsson H A, Trägardh J, Dick K A, Statkute G, Ramvall P, Deppert K and Samuelson L 2008 Precursor evaluation for *in situ* InP nanowire doping *Nanotechnology* **19** 445602
[6] Tomioka K, Motohisa J, Hara S, Hiruma S and Fukui T 2010 GaAs/AlGaAs core multi shell nanowire-based light-emitting diodes on Si *Nano Lett.* **10** 1639–44
[7] Colombo C, Heiß M, Grätzel M and Fontcuberta i Morral A 2009 Gallium arsenide p-i-n radial structures for photovoltaic applications *Appl. Phys. Lett.* **94** 173108
[8] Svensson C P T, Martensson T, Trägardh J, Larsson C, Rask M, Hessman D, Samuelson L and Ohlsson J 2008 Monolithic GaAs/InGaP nanowire light emitting diodes on silicon *Nanotechnology* **19** 305201
[9] Kim H-M, Cho Y-H, Lee H, Kim S I, Ryu S R, Kim D Y, Kang T W and Chung K S 2004 High-brightness light emitting diodes using dislocation-free indium gallium nitride/gallium nitride multiquantum-well nanorod arrays *Nano Lett.* **4** 1059–62
[10] Givargizov E I 1975 Fundamental aspects of VLS growth *J. Cryst. Growth* **31** 20–30
[11] Haraguchi K, Katsuyama T, Hiruma K and Ogawa K 1992 GaAs p–n junction formed in quantum wire crystals *Appl. Phys. Lett.* **60** 745–7
[12] Haraguchi K, Katsuyama T and Hiruma K 1994 Polarization dependence of light emitted from GaAs p–n junctions in quantum wire crystals *J. Appl. Phys.* **75** 4220–5

[13] Gutsche C, Regolin I, Blekker K, Lysov A, Prost W and Tegude F-J 2009 Controllable p-type doping of GaAs nanowires during vapor–liquid–solid growth *J. Appl. Phys.* **105** 024305

[14] Gutsche C, Lysov A, Regolin I, Blekker K, Prost W and Tegude F-J 2010 n-type doping of vapor–liquid–solid grown GaAs nanowires *Nanoscale Res. Lett.* doi:10.1007/s11671-010-9815-7

[15] Joyce H J, Gao Q, Tan H H, Jagadish C, Kim Y, Zhang X, Guo Y and Zou J 2007 Twin-free uniform epitaxial GaAs nanowires grown by a two-temperature process *Nano Lett.* **7** 921–6

[16] Regolin I, Gutsche C, Lysov A, Blekker K, Li Z-A, Spasova M, Prost W and Tegude F-J 2010 Axial pn-junctions formed by MOVPE using DEZn and TESn in vapour–liquid–solid grown GaAs nanowires *J. Cryst. Growth* doi:10.1016/j.jcrysgro.2010.08.028

[17] Chen H D, Feng M S, Chen P A, Lin K C and Wu C C 1994 Low-temperature luminescent properties of degenerate p-type GaAs grown by low-pressure metalorganic chemical vapor deposition *J. Appl. Phys.* **75** 2210–4

[18] Borghs G, Bhattacharyya K, Deneffe K, van Mieghem P and Mertens R 1989 Band-gap narrowing in highly doped n- and p-type GaAs studied by photoluminescence spectroscopy *J. Appl. Phys.* **66** 4381–6

[19] Pankove J I 1971 *Optical Processes in Semiconductors* (New York: Dover)

[20] Nathan M I and Morgan T N 1966 Excitation dependence of photoluminescence in n- and p-type compensated GaAs *Proc. Int. Conf. on Quantum Electronics* p 478

[21] Pankove J I 1962 Tunneling-assisted photon emission in gallium arsenide pn junctions *Phys. Rev. Lett.* **9** 283–5

[22] Casey H C and Silversmith D J 1969 Radiative tunneling in GaAs abrupt asymmetrical junctions *J. Appl. Phys.* **40** 241–56